Reith, M., & Cattolico, R. A. (1985b) *Nature (London)* (submitted for publication).
Reith, M., & Cattolico, R. A. (1985) *Biochemistry* (preceding paper in this issue).
Schiff, J. A. (1971) in *Autonomy and Biogenesis in Mitochondria and Chloroplasts* (Boardman, N. K., Linnane, A. W., & Smillie, R. W., Eds.) pp 98–118, North-Holland, Amsterdam.
Steinmuller, K., Kaling, M., & Zetsche, K. (1983) *Planta 159*, 308–313.
Stewart, W. D. (1974) *Botanical Monographs*, Vol. 10, p 989, University of California Press, Berkeley.
Taylor, F. J. R. (1979) *Proc. R. Soc. London 204*, 267–286.
Towbin, H., Staehelin, T., & Gordon, J. (1979) *Proc. Natl. Acad. Sci. U.S.A. 76*, 4350–4354.
Whatley, J. M. (1983) *Inter. Rev. Cytol. 14*, 329–373.
Whatley, J. M., & Whatley, F. R. (1981) *New Phytol. 87*, 233–247.
Wheeler, A. M., & Hartley, M. R. (1975) *Nature (London) 257*, 66–67.
Whitfeld, P. R., & Bottomley, W. (1983) *Annu. Rev. Plant Physiol. 34*, 279–310.
Wildman, S. G. (1982) in *The Origin of Chloroplasts* (Schiff, J., Ed.) pp 229–242, Elsevier/North-Holland, New York.
Zielinski, R. E., & Price, C. A. (1980) *J. Cell Biol. 85*, 435–445.

# Changes in Protein Conformation and Stability Accompany Complex Formation between Human C1 Inhibitor and $C1\bar{s}$[†]

Michael Lennick, Shelesa A. Brew, and Kenneth C. Ingham*
*Plasma Derivatives Laboratory, American Red Cross Blood Services Laboratories, Bethesda, Maryland 20814*
*Received August 21, 1984*

ABSTRACT: The fluorescence spectrum of C1 inhibitor (C1-Inh) in aqueous buffer has a maximum at 324 nm which shifts to 358 nm in 6.0 M guanidinium chloride (GdmCl), indicating that fluorescent tryptophans are buried in the native protein. When titrated with GdmCl, the fluorescence intensity, polarization, and emission maximum of C1-Inh and $C1\bar{s}$ exhibited clear transitions which were more prominent than those of the enzyme–inhibitor complex. Two of the variables (intensity and emission maximum) suggest biphasic unfolding of C1-Inh. Differential absorption measurements and sodium iodide quenching of intrinsic fluorescence were consistent with a net increase in the exposure of tryptophans and tyrosines upon complex formation. This reaction, i.e., complex formation, was also accompanied by an increase in the ability to enhance the fluorescence of the hydrophobic probe 8-anilino-1-naphthalenesulfonate. Fluorescence assays of heat denaturation showed transitions at 40 and 52 °C for $C1\bar{s}$ and at 60 °C for C1-Inh whereas there was no detectable melting transition for the complex. Similarly, differential scanning calorimetric measurements revealed transitions at 42, 52, and 62 °C for $C1\bar{s}$ and one transition at 60 °C for C1-Inh, with no major transitions detectable for the complex. The ratio of the calorimetric enthalpy to the apparent van't Hoff enthalpy for thermal unfolding of C1-Inh was 1.6. Taken together, these results suggest that C1-Inh and $C1\bar{s}$ are each composed of at least two independently unfolding domains and that complex formation, which involves conformational change, yields a protein substantially more stable than either component alone.

C1 inhibitor (C1-Inh),[1] the only circulating protease inhibitor known to react with the activated complement components $C1\bar{r}$ and $C1\bar{s}$ (Sim et al., 1979; Ziccardi, 1981), plays a crucial role in the control of the plasma complement cascade. This is illustrated by the sometimes severe medical symptoms displayed by individuals with inherited deficiencies of this protein (Donaldson & Evans, 1963). Native human C1-Inh is a single-chain glycoprotein with three disulfide bonds and an amino acid composition which is unremarkable except for its relatively low tryptophan and tyrosine contents (Haupt et al., 1970). Up to 35% of the inhibitor's 104000 molecular weight is composed of sugar residues (Haupt et al., 1970; Harrison, 1983), making this one of the most heavily glycosylated plasma proteins. The limited information available about C1-Inh three-dimensional structure comes from the circular dichroic spectrum which indicates that the C1-Inh secondary structure is composed of nearly equal proportions of $\alpha$-helix, $\beta$-sheet, and aperiodic structure (Nilsson et al., 1983) and from electron microscopic visualization of the rotary-shadowed molecule which appears to consist of a globular domain 40 Å in diameter attached to the end of a rod-shaped domain, 330 Å long and 20 Å in diameter (Odermatt et al., 1981). In the past several years, it has been shown that C1-Inh reacts with $C1\bar{r}$ and $C1\bar{s}$ to form stoichiometric 1:1 complexes

[†] Publication No. 629 from the American Red Cross Blood Services Laboratories, Bethesda, MD. A preliminary account has appeared in abstract form (Lennick et al., 1983). This work was supported in part by Grant HL-21791 from the National Institutes of Health.

[1] Abbreviations: ANS, 8-anilino-1-naphthalenesulfonate; DSC, differential scanning calorimetry; P, polarization; Cbz-Lys-sBzl, $N^{\alpha}$-carbobenzyloxy-L-lysine thiobenzyl ester; HPSEC, high-performance size-exclusion chromatography; SDS, sodium dodecyl sulfate; DTDP, 4,4′-dithiodipyridine; PBS, phosphate-buffered saline; C1-Inh, C1 inhibitor; GdmCl, guanidinium chloride; bis(ANS), 5,5′-bis[8-(phenylamino)-1-naphthalenesulfonate]; Tris, tris(hydroxymethyl)aminomethane; $Me_2SO$, dimethyl sulfoxide.

0006-2960/85/0424-2561$01.50/0 © 1985 American Chemical Society

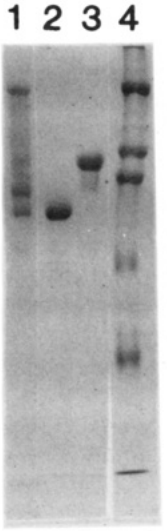


FIGURE 1: SDS–polyacrylamide gel electrophoresis of nonreduced samples of C1-Inh/C1$\bar{s}$ complex (lane 1), C1$\bar{s}$ (lane 2), and C1-Inh (lane 3). The reduced molecular weight standards (lane 4) are myosin (205 000), $\beta$-galactosidase (116 000), phosphorylase (97 400), bovine serum albumin (66 000), and ovalbumin (45 000).

(Harpel & Cooper, 1975; Arlaud et al., 1979; Ziccardi & Cooper, 1979). The fact that these complexes are stable to heat and SDS but are not stable to hydroxylamine hydrolysis (Chesne et al., 1982) suggests a covalent ester linkage. The object of this paper is to present the results of a series of experiments designed to detect changes in structure and stability induced by covalent complex formation between C1-Inh and C1$\bar{s}$. Such changes are thought to be functionally important for the recognition, degradation, and clearance of inactive protein complexes in the blood (Villanueva & Danishefsky, 1979; Gonias et al., 1983).

## Materials and Methods

The substrate for the esterolytic assay, Cbz-Lys-sBzl, was purchased from Vega Biochemicals. The chromogen 4,4′-dithiodipyridine (DTDP) was purchased from Sigma. 8-Anilino-1-naphthalenesulfonic acid (ANS), free of bis(ANS), was purchased from Molecular Probes. Sepharose 4B was purchased from Pharmacia. Cyanogen bromide was purchased from Eastman. Guanidine hydrochloride was purchased from Heico. All other chemicals were purchased from Sigma. Hexyl-Sepharose was made by activating Sepharose 4B with cyanogen bromide as described by Kolb et al. (1979), followed by coupling with hexylamine as described by Nilsson & Wiman (1982). Sodium dodecyl sulfate–polyacrylamide slab gel electrophoresis was performed on 8% polyacrylamide slab gels according to the method of Laemmli (1970). Protein samples were prepared for electrophoresis by incubation with 5% (w/v) SDS for 30 min at 37 °C.

Purified C1$\bar{s}$ was a generous gift from Dr. David H. Bing. This preparation displayed a single Coomassie blue stained band of about 85 000 daltons (nonreduced) in SDS slab gel electrophoresis (Figure 1, lane 2) and a single peak by HPSEC. C1$\bar{s}$ concentrations were determined optically by assuming $A^{1\%}_{280nm}$ = 10.0 cm$^{-1}$ and $M_r$ = 83 000 (Sim et al., 1977).

The source of C1-Inh was a preparation of intermediate purity (20%) supplied by Dr. Milan Wickerhauser (Wickerhauser, 1980). C1-Inh was purified to homogeneity by modification of the procedures of Nilsson & Wiman (1982). Five hundred milligrams of the intermediate purity preparation (equivalent to 50 mg of C1-Inh) was dissolved in 10 mL of ice-cold 40 mM sodium phosphate, pH 7.0. The solution was made 1.7 M in ammonium sulfate by slow addition of a concentrated stock solution at 0 °C. The precipitate was discarded, and supernatant was loaded onto a 3.8 cm × 20 cm hexyl-Sepharose column previously equilibrated with 40 mM sodium phosphate and 1.7 M $(NH_4)_2SO_4$, pH 7.0 at 4 °C. The column was developed with a decreasing linear salt gradient composed of 350 mL of 1.7 M $(NH_4)_2SO_4$ and 350 mL of 0.4 M $(NH_4)_2SO_4$, both 40 mM in sodium phosphate, pH 7.0, and 0.02% in sodium azide. Fractions exhibiting high C1-Inh activity were pooled and stored in solution at 4 °C until needed (up to several months). C1-Inh concentrations were determined optically by assuming $A^{1\%}_{280nm}$ = 4.5 cm$^{-1}$ and $M_r$ ~ 104 000 (Haupt et al., 1970) and by titrations of C1$\bar{s}$ esterolytic activity as described below. Overloaded SDS gels of purified C1-Inh showed a main band of $M_r$ ~111 000 with some batches containing small amounts of lower molecular weight contaminants (Figure 1, lane 3). Material to be used in fluorescence measurements was further purified by HPSEC.

C1-Inh/C1$\bar{s}$ complex was prepared by adding a 5% molar excess of C1-Inh to a solution of C1$\bar{s}$ and incubating for 15 min at room temperature. HPSEC was used to assess the yield and homogeneity of the product and, in the case of material to be used for fluorescence measurements, to separate the complex from residual unreacted components (Ingham et al., 1983). This purification step also served to remove the modified inhibitor (I*) first described by Weiss & Engel (1983) which appeared as a 90 000-dalton band on nonreduced SDS gels (lane 1, Figure 1). The amounts of I* formed varied from batch to batch. Analysis by HPSEC indicated that the batches used for DSC measurements contained less than 10% of I* and/or unreacted components. Once purified by exclusion chromatography, the complex appeared to be stable for several hours at room temperature or several days at 4 °C as judged by the absence of significant dissociation products in subsequent SDS gels or HPSEC profiles.

C1-Inh activity and the extent of complex formation with C1$\bar{s}$ were also determined by the inhibition of C1 esterase activity in a kinetic assay using a synthetic peptide thio ester substrate, Cbz-Lys-sBzl, in combination with the chromogenic thiol reagent DTDP as described by McRae et al. (1981). The buffer used in all assays was 0.1 M Tris, 0.1 M NaCl, and 9.2% $Me_2SO$, pH 7.4. All assays were performed at 30 °C in a Cary 118 double-beam recording spectrophotometer with thermostated cell holders. Stock solutions of chromogen (2 mM dithiodipyridine in assay buffer) and substrate (2 mM Cbz-Lys-sBzl in deionized water and 9.2% $Me_2SO$) were prepared in advance. Buffer, chromogen (0.3 mM final concentration), and substrate (0.12 mM final concentration) were mixed in a 1 cm$^2$ quartz cuvette and allowed to equilibrate to temperature. Blanks, containing buffer, chromogen, and substrate, were prepared for each assay. For titrations, aliquots of different dilutions of C1-Inh solution were added to aliquots of active C1$\bar{s}$ in wells of plastic microtitration plates. The contents were mixed by shaking and incubated for 15 min at room temperature. Esterolysis was initiated by adding C1$\bar{s}$ or the C1$\bar{s}$/C1-Inh mixtures (6.3 nM final C1$\bar{s}$ concentration) to the sample cuvette and was monitored by the increase in absorbance at 324 nm (Castillo et al., 1979). The velocity ($v$) of the enzyme-catalyzed reaction, determined from the slope of the plot of absorbance vs. time, was proportional to the concentration of free enzyme.

High-performance size-exclusion chromatography (HPSEC) was performed at room temperature using an 0.8 × 30 cm size exclusion column (TSK G3000SW, Varian) equilibrated with 40 mM sodium phosphate, 150 mM NaCl, and 0.02% sodium

azide, pH 7.0 (PBS). All buffers were sterile filtered and extensively degassed prior to use. Samples were injected with a Waters U6K injector, and protein elution was monitored at 280 nm with a Waters Model 450 variable-wavelength detector.

Fluorescence measurements were made with a Perkin-Elmer MPF-4 fluorescence spectrophotometer fitted with a temperature-controlled cell block connected to a circulating water bath with a proportional temperature controller. For thermal stability studies, the proportional controller was set to maintain a constant heating rate of 1 °C/min. For all measurements reported here, the fluorometer was set to ratio mode, and the excitation and emission slits were set at 10 nm.

Fluorescence polarizations were calculated according to

$$P = (I_{vv} - GI_{vh})/(I_{vv} + GI_{vh}) \quad (1)$$

where $I_{vv}$ and $I_{vh}$ are the intensities of protein fluorescence excited with vertically polarized light (295 nm) and detected with the emission polarizer in the vertical and horizontal orientations, respectively. $G$, a correction factor due to polarization induced by gratings in the fluorometer, is equivalent to $I_{hv}/I_{hh}$, the ratio of the intensities of horizontally excited protein fluorescence detected with the emission polarizer in the vertical and horizontal orientations.

Fluorescence quenching experiments were done by titrating the protein solutions with small volumes of a 5 M NaI solution and measuring the intrinsic fluorescence at 25 °C. The buffer in all quenching experiments was PBS. Emission was measured at 333, 327, and 332 nm for C1$\bar{s}$, C1-Inh, and the C1$\bar{s}$/C1-Inh complex, respectively, with excitation at 295 nm. The absorbance at 295 nm never exceeded 0.1 to minimize inner filter effects, and all measurements were corrected for light-scattering and dilution effects. The iodide quenching data were analyzed by the modified Stern–Volmer equation (Lehrer, 1971)

$$F_0/\Delta F = 1/([Q]f_aK_a) + 1/f_a \quad (2)$$

where $F_0$ is the fluorescence intensity in the absence of quencher, $\Delta F$ ($=F_0 - F$) is the total change in fluorescence at quencher concentration [Q], $f_a$ is the fraction of fluorescence originating from residues which are accessible to the quencher, and $K_a$ is the average quenching constant of the accessible fluorophore population.

Thermal unfolding studies using intrinsic and ANS fluorescence were done with 0.84 $\mu$M solutions of C1$\bar{s}$, C1-Inh, and C1$\bar{s}$/C1-Inh complex in PBS. Excitation/emission wavelengths were 280/330 nm for the intrinsic fluorescence measurements and 400/480 nm for experiments done in the presence of 60 $\mu$M ANS. To estimate apparent van't Hoff enthalpies for thermal denaturation as monitored by ANS fluorescence, the fraction of protein denatured, $f_D$, was calculated by interpolation along the melting curve as follows:

$$f_D = \frac{F - F_N}{F_D - F_N} \quad (3)$$

where $F$ is the observed fluorescence intensity at any temperature in the region of the transition and $F_N$ and $F_D$ are the fluorescence intensities of the native and denatured states, respectively, taken as lowest and highest intensities in the melting curve. The resulting values of $f_D$ were used to calculate apparent equilibrium constants for denaturation as a function of temperature from the expression $K_D = f_D/(1 - f_D)$. Values of $f_D$ less than 0.1 and greater than 0.9 were discarded. The apparent van't Hoff enthalpies were determined from the slopes of plots of log $K_D$ vs. inverse temperature. Melting temperatures were determined by the point at which log $K_D$ was equal to zero.

The UV difference spectrum, due to C1$\bar{s}$/C1-Inh complex formation, was obtained by using a Cary 118 scanning spectrophotometer with an expanded scale and a strip chart recorder. The protein in PBS was placed in 1 cm$^2$ tandem quartz absorption cells at concentrations of 7.7 $\mu$M, providing a total absorbance at 280 nm of approximately 1.0 in the loaded cells (Donovan, 1969).

Differential scanning calorimetry was done with a MicroCal MC-1 scanning calorimeter equipped with Chromalloy cylindrical sample cells. Tracings of individual scans were recorded with a Houston Instrument Omnigraphic 2000 X-Y recorder. Protein concentrations ranged from 3 to 9 mg/mL. Transition base lines for C1-Inh were approximated by extending the pre- and posttransition base lines through the transition and connecting them with a vertical line dropped from the midpoint, as indicated by the dashed line in Figure 9. Transition base lines for C1$\bar{s}$ were approximated by joining the pre- and posttransition base lines with a straight line. Heats of unfolding were determined by comparison of peak areas to those obtained with known heats supplied by calibration currents. Integrations of calibration heats and heats of unfolding were performed by tracing the calorimeter outputs onto high-quality tracing paper, cutting out the appropriate areas, and weighing them on an analytical balance. Each $\Delta H_{cal}$ presented is an average of at least two such determinations. The apparent van't Hoff enthalpy for C1-Inh was calculated according to the equation (Privalov & Medved, 1982):

$$\Delta H_{vH} = 4RT_m^2C_{max}/Q \quad (4)$$

where $R$ is the gas constant, $T_m$ is the temperature of the midpoint of the thermal transition, $C_{max}$ is the maximal excess heat capacity, and $Q$ is the calorimetrically determined enthalpy.

Due to uncertainties involved in determining the base lines and areas of individual thermal transitions of C1$\bar{s}$, unambiguous assignments of $\Delta H_{vH}$ could not be made by using eq 4; depending on the choices made, ratios of $\Delta H_{cal}/\Delta H_{vH}$ ranged between 0.5 and 1.3 for the 52 °C endotherm.

## RESULTS

*Unfolding in Guanidine.* The fluorescence spectra of equimolar solutions of C1-Inh, C1$\bar{s}$, and the C1-Inh/C1$\bar{s}$ complex, in the absence and presence of 6 M GdmCl, are shown in Figure 2. The fluorescence of C1-Inh has a maximum at 324 nm which is red shifted to 358 nm and is highly quenched in 6 M GdmCl. The maximum for C1$\bar{s}$ is shifted less, from 332 to 353 nm, and shows less apparent quenching as a result of unfolding in GdmCl. The fluorescence maximum of the complex is intermediate between those of C1-Inh and C1$\bar{s}$ and shows less of a shift, 329 to 340 m, and less quenching in 6 M GdmCl than either of the components. In the absence of GdmCl, the integrated fluorescence intensity of the complex is about 9% less than the sum of the individual components. A decrease of similar magnitude was recently reported for the complex between thrombin and antithrombin III (Wong et al., 1983).

The dependence of intrinsic fluorescence properties (polarization, relative intensity, and emission maximum) on GdmCl concentration is shown in Figure 3. The total changes in each of the three variables are much less for the complex than for either the protease or the inhibitor, and distinct transitions are not apparent. In the case of the inhibitor, two of the variables, intensity and emission maximum, show bi-

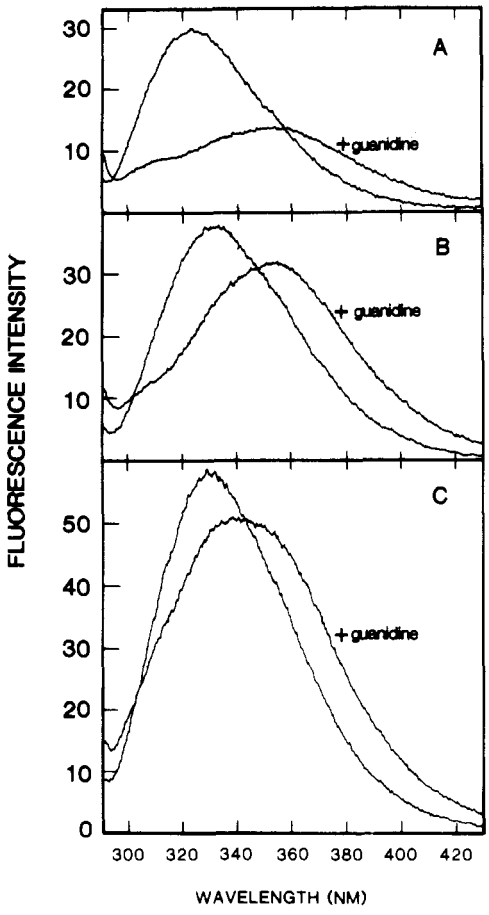


FIGURE 2: Fluorescence spectra of C1-Inh (A), C1s̄ (B), and the C1-Inh/C1s̄ complex (C) before and after equilibration with 6 M GdmCl. Fluorescence spectra were measured at the same instrument settings with excitation at 295 nm at protein concentrations of 0.4 μM in PBS in the presence and absence of 6 M GdmCl.

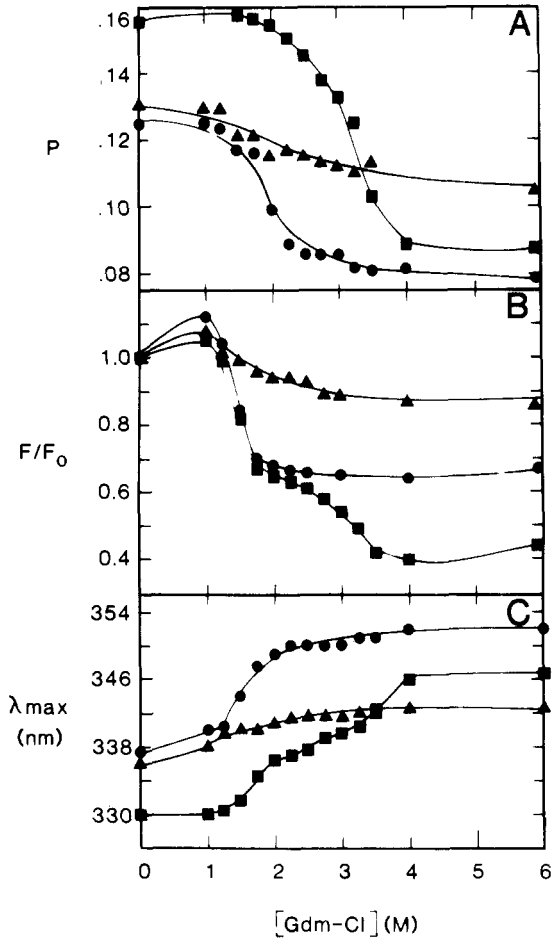


FIGURE 3: Effects of GdmCl concentration on intrinsic fluorescence variables of C1-Inh, C1s̄, and the C1-Inh/C1s̄ complex. Trp fluorescence polarization (A), relative fluorescence intensity at 330 nm (B), and the wavelength maximum (C) were measured for 0.4 μM solutions of C1-Inh (■), C1s̄ (●), and the C1-Inh/C1s̄ complex (▲) in PBS with various concentrations of GdmCl at 295-nm excitation. Aliquots of concentrated protein solutions were mixed with buffer and 8 M GdmCl to yield the desired final GdmCl concentrations and incubated for 2 h at room temperature prior to making measurements.

phasic behavior; one transition occurs between 1 and 2 M GdmCl (with no change in polarization) while the second occurs between 2 and 4 M GdmCl. With C1s̄, all three parameters show single transitions between 1 and 2 M GdmCl.

*Exposure of Aromatic Side Chains.* Sodium iodide quenching of intrinsic fluorescence was analyzed according to the modified Stern–Volmer equation (Lehrer, 1971). The linearity of the plots in Figure 4 supports the notion that the fluorescent tryptophans of each protein can be divided into two groups: those which are sufficiently exposed to solvent to be collisionally quenched by iodide and those which are not. The fraction of fluorescence derived from exposed residues, as calculated from the $y$ intercepts in Figure 4, was 0.13 for the inhibitor, 0.23 for C1s̄, and 0.25 for the complex. The latter value is well above the weighted average of the first two, consistent with a net exposure of tryptophans upon complex formation.

Additional data related to the disposition of aromatic side chains come from the differential absorption measurements shown in Figure 5. The negative bands at 278 and 286 nm are consistent with a polarization blue shift experienced by tyrosines exposed to solvent whereas that at 294 nm is consistent with a similar exposure of tryptophans (Donovan, 1969). Using Donovan's estimates of $\Delta\epsilon(292\text{ nm}) = 1600\ M^{-1}$ for tryptophan and $\Delta\epsilon(287\text{ nm}) = 700\ M^{-1}$ for tyrosine and correcting for the contribution of tryptophan to the tyrosine peak by using $\Delta\epsilon(287\text{ nm}) = 900\ M^{-1}$ for tryptophan, our data are equivalent to the transfer of 1.4 tyrosines and 1.1 tryptophan residues from a completely buried to a completely exposed environment upon complex formation. In fact, the transfer of a larger number of chromophores from partially exposed to more exposed environments could produce a similar effect. However, the sign of the difference spectrum is consistent only with a net increase in polarity of the environment of one or more tryptophans and one or more tyrosines. The difference spectrum was completely developed within 5 min of mixing, and no further time-dependent changes were observed within 2 h.

*Thermal Denaturation: (A) Fluorescence.* The temperature dependence of tryptophan fluorescence for C1-Inh, C1s̄, and the C1-Inh/C1s̄ complex is shown in Figure 6. There is a steady decline with increasing temperature for all three samples. C1-Inh displays a single irreversible transition at about 60 °C. The pattern of C1s̄ fluorescence is more complex with a plateau region between 35 and 40 °C and a more obvious transition at about 52 °C. However, the complex displays no clear transition.

Thermal denaturation was also monitored by use of the hydrophobic fluorescent probe ANS (Weber & Laurence, 1954; Gally & Edelman, 1965; Busby et al., 1981). As shown in Figure 7, the ANS fluorescence detected clear transitions for C1-Inh and C1s̄ at 60 and 52 °C, respectively. In addition, another small-amplitude transition was seen for C1s̄ near 40

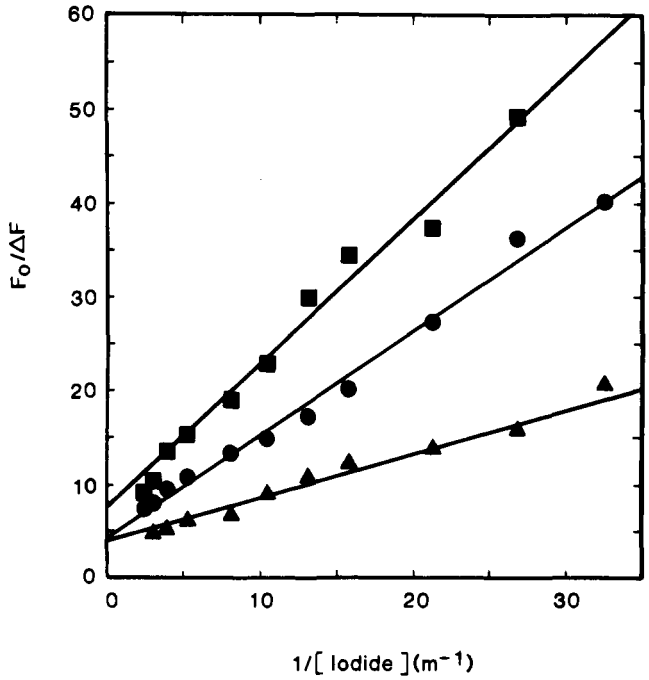


FIGURE 4: Iodide quenching of intrinsic tryptophan fluorescence of C1-Inh (■), C1$\bar{s}$ (●), and the C1-Inh/C1$\bar{s}$ complex (▲). Small aliquots of a 5 M NaI solution were added to 1-mL samples of proteins at 0.4 $\mu$M in PBS at 25 °C. Excitation of fluorescence was at 295 nm. The solid lines are fitted to the data according to the modified Stern–Volmer equation (eq 2 in the text).

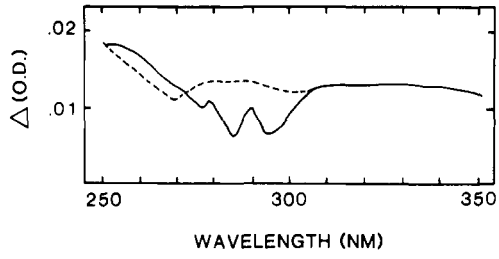


FIGURE 5: Differential UV absorbance spectrum of complex formation between C1-Inh and C1$\bar{s}$. The spectrum was obtained by mixing 0.75 mL of 7.7 $\mu$M C1$\bar{s}$ with an equal volume of 7.7 $\mu$M C1-Inh, both in PBS at 25 °C, in a tandem 1 cm$^2$ quartz cuvette. The solid line is the difference spectrum while the dashed line is a protein–protein base line obtained before the sample was mixed.

°C. In contrast, no definite melting transitions were observed for the heated complex, whose initial fluorescence was higher than that of either component alone. van't Hoff analysis of a series of similar experiments was used to determine the effect of heating rate on the enthalpy of denaturation for C1-Inh. The apparent $\Delta H_{vH}$ values were 128, 107, and 118 kcal/mol, with corresponding midpoints of 60, 60, and 63 °C at scan rates of 0.5, 1.0, and 1.7 °C/min, respectively.

Upon cooling, none of the samples in the experiments shown in Figure 6 or Figure 7 returned to the original fluorescence intensity. This is reflected in the ratios of the fluorescence intensities before heating to those after heating (Table I). This implies that some irreversible damage has occurred in the complex as well as in the enzyme and in the inhibitor. However, the relatively small change in ANS fluorescence for the complex suggests much less unfolding and/or aggregation than with the isolated components.

(*B*) *HPSEC.* Additional experiments were performed to determine the extent to which increases in ANS fluorescence correlate with changes in elution behavior. Solutions containing protein at 0.2 mg/mL were heated at 1 °C/min while the ANS fluorescence of separate identical samples containing

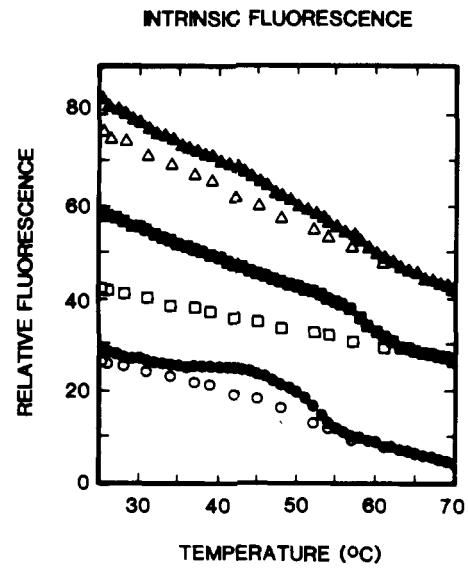


FIGURE 6: Dependence of intrinsic fluorescence intensity on temperature. C1-Inh (■), C1$\bar{s}$ (●), and the C1-Inh/C1$\bar{s}$ complex (▲) at 0.4 $\mu$M in PBS were heated (closed symbols) and then cooled (open symbols) at 1 °C/min. Excitation/emission wavelengths were 280/330 nm. Some of the curves have arbitrarily been displaced along the *y* axis in order to facilitate viewing.

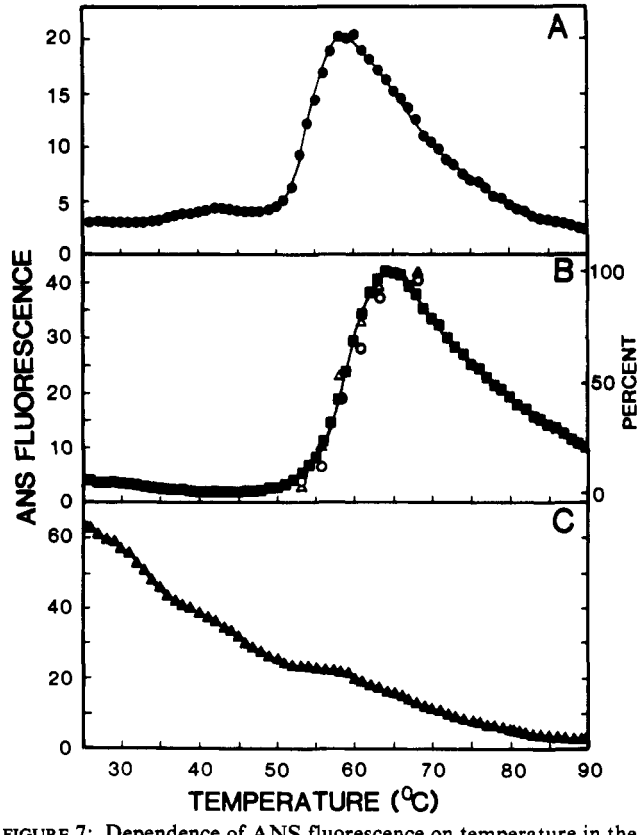


FIGURE 7: Dependence of ANS fluorescence on temperature in the presence of C1$\bar{s}$ (A), C1-Inh (B), and the C1-Inh/C1$\bar{s}$ complex (C). Solutions containing protein at 0.8 $\mu$M in PBS were heated at 1 °C/min in the presence of 60 $\mu$M ANS. The open symbols in panel B represent the percent loss of activity (Δ) and the percent conversion to the fast-eluting form (○) of C1-Inh samples withdrawn at the indicated temperatures (see text).

the dye was simultaneously monitored. Aliquots were removed at various temperatures, quickly cooled to room temperature, and subsequently analyzed by HPSEC and, in the case of C1-Inh, for the ability to inhibit C1$\bar{s}$. As shown in Figure 8, all three proteins eluted as single peaks prior to heating. With C1-Inh, material eluting at or near the void could be detected

Table I: Thermal Denaturation Parameters for C1 Inhibitor, C1s̄, and the C1-Inh/C1s̄ Complex

| protein | $T_m$ (°C) Trp | $T_m$ (°C) ANS | $T_m$ (°C) DSC | fluorescence ratio[a] Trp | fluorescence ratio[a] ANS | $\Delta H_{cal}$ (kcal/mol), DSC | $\Delta H_{vH}$ (kcal/mol) DSC | $\Delta H_{vH}$ (kcal/mol) ANS |
|---|---|---|---|---|---|---|---|---|
| C1-Inh | 60 | 60 | 60 | 0.66 | 32.5 | 192 | 121 | 111[c] |
| C1s̄ | ~40, 52 | ~40, 52 | 42, 52, 62[b] | 0.94 | 51.2 | 324[d] | | 207[e] |
| complex | | | | 0.90 | 2.2 | | | |

[a] Fluorescence ratio = ratio of fluorescence intensity after heating to that before heating as in Figures 6 and 7. [b] Commas denote multiple transitions. [c] Average of three values obtained at heating rates of 0.5, 1.0, and 1.7 °C/min. [d] Calculated for the total heat between the calorimetric curve and the dashed base line in Figure 9. [e] Value given is for the 52 °C transition.

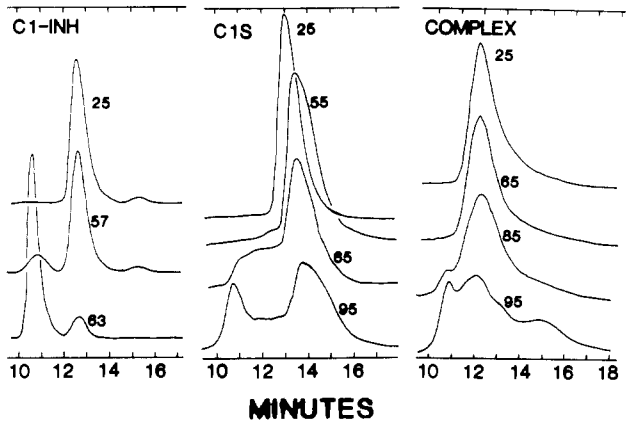


FIGURE 8: High-pressure size-exclusion chromatography of C1-Inh, C1s̄, and the C1-Inh/C1s̄ complex after heating to various temperatures. Solutions containing the proteins at 0.2 mg/mL in PBS were heated at 1 °C/min. Samples were withdrawn at the indicated temperatures, quickly cooled to room temperature, and injected onto the column which was pumped at 0.5 mL/min. The 95 °C sample of the complex was kept at 4 °C overnight before HPSEC.

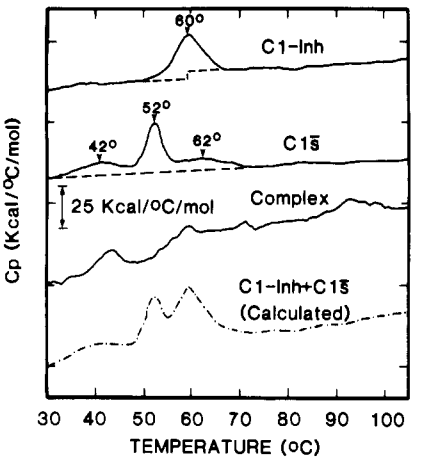


FIGURE 9: Differential scanning calorimetry of C1-Inh, C1s̄, and the C1-Inh/C1s̄ complex. The top three curves are averages of at least two calorimetry experiments each for C1-Inh, C1s̄, and the C1-Inh/C1s̄ complex. The bottom curve is calculated to predict the heat absorption pattern expected for the complex in the absence of any effects due to protein–protein interactions. The dahsed lines represent base lines used in estimating $\Delta H$'s (see Materials and Methods).

in the sample withdrawn at 57 °C, shortly after the onset of the increase in fluorescence (Figure 7B). The sample withdrawn at 63 °C, near the completion of the ANS-detected transition, was almost 90% converted to the fast-eluting form. The open symbols in Figure 7B show that the changes in elution behavior as well as the loss of inhibitory activity correlated closely with the increase in ANS fluorescence.

Changes in the elution pattern of C1s̄ were more complex than for C1-Inh. As shown in Figure 8, the sample withdrawn at 55 °C was significantly retarded and broadened compared to the unheated control. Although not shown, this phenomenon could also be detected in a sample withdrawn at 45 °C but not at 35 °C, suggesting that the small inflections near 40 °C in the ANS (and tryptophan) fluorescence vs. temperature curves signify actual changes in the protein. Further heating caused the appearance of faster eluting material, but the extent of unfolding and/or aggregation was less than with C1-Inh and appeared to lag behind the major rise in ANS fluorescence. Even after heating to 95 °C, only about one-fourth of the material appeared in the void while with C1-Inh the conversion was complete by 68 °C.

The C1-Inh/C1s̄ complex, which showed no obvious thermal transitions by fluorescence, was also more stable in terms of its elution behavior. Although samples were withdrawn every 10 °C, a change in the profile was not detected until 75 °C, well beyond the temperature range where the isolated constituents exhibit fluorescence transitions as well as changes in elution behavior. The sample withdrawn at 85 °C (Figure 8) showed definite signs of unfolding and/or aggregation which was compounded by further heating to 95 °C where dissociation or fragmentation into slower moving components was also evident. These changes might be related to the lack of complete reversibility of fluorescence parameters.

(*C*) *Calorimetry.* Differential scanning calorimetric measurements are summarized in Figure 9 and Table I. C1-Inh shows a single broad transition with $\Delta H_{cal}$ = 192 kcal/mol (1.8 cal/g) and a midpoint of 60 °C, identical with that of the transitions seen by fluorescence. Analysis of the melting profile by eq 4 yields an apparent van't Hoff enthalpy of 121 kcal/mol, also in good agreement with the values calculated from the ANS experiments. The corresponding $\Delta H_{cal}/\Delta H_{vH}$ ratio for C1-Inh is 1.6. The C1s̄ thermogram shows a prominent peak at 52 °C and less distinct but reproducible features near 42 and 62 °C with a total $\Delta H_{cal}$ = 198 kcal/mol (3.9 cal/g). The 42 and 52 °C transitions have their counterpart in the fluorescence curves, but the one at 62 °C is seen only by DSC. These transitions, except possibly the one occurring at 42 °C in the C1s̄ thermogram, either are missing or are of diminished amplitude in the complex. The lowest curve in Figure 9 was calculated to predict the heat absorption profile expected for the complex in the absence of any effects due to protein–protein interactions. Analysis by HPSEC indicated that in all three cases the elution of the proteins shifted to the void of the column after heating to 106 °C in the calorimeter. The greater extent of aggregation relative to that depicted in Figure 8 can be attributed to the 10–40-fold higher protein concentrations and the higher temperatures reached in the calorimeter.

## Discussion

Two types of thermodynamic variables can potentially be derived from calorimetric experiments such as those reported here. The first, $\Delta H_{cal}$ is related to the total amount of heat absorbed during a melting transition, as measured by the area under the calorimetric curve. The second, $\Delta H_{vH}$, relates to

the shape of the melting transition. Sharp transitions are characterized by larger $\Delta H_{vH}$ values than broad transitions. For a two-state reversible process, the ratio of $\Delta H_{cal}$ to $\Delta H_{vH}$ should be close to unity, and this has been found for the melting of some small reversibly unfolding proteins [reviewed in Privalov (1979)]. The fact that larger proteins frequently exhibit $\Delta H_{cal}/\Delta H_{vH}$ ratios greater than 1 has been attributed to the occurrence of stable intermediates in the unfolding or to the existence of multiple domains whose independent melting transitions are too close to be resolved but sufficiently separated to broaden the shape of the endotherm (Freire & Biltonen, 1978; Privalov, 1982).

Two separate lines of evidence presented here are consistent with the occurrence of independently unfolding doamins in C1-Inh. First the $\Delta H_{cal}/\Delta H_{vH}$ ratio of 1.6 is not compatible with a single two-state transition. Even though the melting of C1-Inh is not reversible, a ratio grater than 1 can still be interpreted as evidence for multiple domains since the factors contributing to irreversibility can only sharpen the endotherm by pulling the reaction toward completion and increasing the apparent $\Delta H_{vH}$ (Privalov, 1982). Furthermore, if aggregation is exothermic (Privalov & Khechinashvili, 1974), this would reduce the amount of heat absorbed, further diminishing $\Delta H_{cal}/\Delta H_{vH}$. Second, the dependence of the intrinsic fluorescence intensity and the emission maximum on GdmCl concentration is clearly biphasic. This result is similar to that reported by Villanueva & Allen (1983) for antithrombin III, a related serum protease inhibitor. The two-domain structure for C1-Inh, which was proposed by Odermatt et al. (1981) on the basis of their electron microscopic studies, is consistent with an interpretation of our data such that the two domains unfold independently and display differential stabilities toward heat and, to a more obvious extent, toward GdmCl.

Differences between denaturation by GdmCl and by heat were also seen with C1$\bar{s}$. The former produced only a single transition whereas the latter was more complex with two unfolding transitions detected by ANS fluorescence and three by scanning calorimetry. Additional DSC and ANS fluorescence experiments show that, in the presence of 5 mM $Ca^{2+}$, where C1$\bar{s}$ dimerizes, the 42 °C feature disappears while the one at 62 °C becomes much more intense (unpublished results). It is therefore possible that the 42 °C transition arises from protein structure affected by $Ca^{2+}$ binding and/or self-association. In this regard, it is interesting to note that a dumbbell-like structure has recently been proposed for the zymogen form of the enzyme, based on hydrodynamic and electron microscopic studies of $C1r_2C1s_2$ complexes (Tschopp et al., 1980). This multidomain architecture is consistent with the pattern seen in many complex proteases where the active site is localized in a single domain with others being required for regulation and interaction with other proteins or cells (Neurath, 1984).

A striking result of the calorimetric and fluorescence measurements presented here is the absence of a clear transition for unfolding of the protease–protease inhibitor complex, either by heat or when titrated with GdmCl, one of the most potent disrupters of tertiary and quaternary interactions (Franks & Eagland, 1975; Pace, 1975). The intrinsic fluorescence maximum of the complex in 6 M GdmCl occurs at a significantly shorter wavelength than that of either component, indicating that unfolding is less complete than in the isolated components under the same conditions. Although the complex failed to completely recover its original tryptophan fluorescence, retained a small increase in the ability to enhance ANS fluorescence, and was significantly aggregated after heating, this required temperatures substantially higher than would be expected if the various domains of C1-Inh and C1$\bar{s}$ retained their independence in the complex. Thus, if an endothermic event accompanies or precedes the heat-induced aggregation reaction, then this transition is either too weak or too broad to be detected by our instrument. There are a number of precedents for protease–protease inhibitor complexes melting at higher temperatures than either component separately (Chlebowski & Williams, 1983; Takahashi & Sturtevant, 1981; Zahnley, 1979, 1980; Donovan & Beardslee, 1975). In the present case, stabilization appears to have been sufficient to shift the major melting transitions beyond the accessible range. This implies the existence of strong protein–protein interactions between the components, beyond that provided by the covalent link between them.

Circular dichroic measurements by Nilsson & Wiman (1983) suggest that very little change in secondary structure accompanies complex formation between C1-Inh and C1$\bar{s}$ but that the environment of tryptophan residues is modified. One might expect this reaction to result in the burial of groups present on the combining surfaces. However, our differential absorption and fluorescence quenching measurements indicate an apparent net exposure of Trp and Tyr side chains. Similar conclusions were reached for the antithrombin–thrombin system (Villanueva & Danishefsky, 1979). Another similarity between these two systems is the much greater enhancement of fluorescence of the hydrophobic dye ANS by complexes relative to that by the individual components [Atha et al., 1984; see Figure 7 of this work]. Thus, increased exposure of nonpolar residues may result in the formation of hydrophobic sites on the surfaces of these complexes. These sites could conceivably play a role in receptor function, facilitating the rapid removal of complexes from circulation (Ohlsson, 1971a,b; Gan, 1979; Fuchs et al., 1982; Shifman & Pizzo, 1982; Gonias et al., 1983). Therefore, the changes in conformation reported here could have a 2-fold functional significance: first, in the mechanism of protease inhibition and, second, in the mechanism(s) of clearance of inactive complexes from the blood.

## ACKNOWLEDGMENTS

We thank Milan Wickerhauser, Ph.D., for providing ample quantities of intermediate-purity C1-Inh. We also thank Dr. David Bing for providing the C1$\bar{s}$ used in this study and for guidance with the spectrophotometric assay.

**Registry No.** C1-Inh, 80295-38-1; C1s, 80295-70-1.

## REFERENCES

Arlaud, G. J., Reboul, A., Sim, R. B., & Colomb, M. G. (1979) *Biochim. Biophys. Acta 576*, 151–162.

Atha, D. H., Brew, S. A., & Ingham, K. C. (1984) *Biochim. Biophys. Acta 785*, 1–6.

Brower, M. S., & Harpel, P. C. (1982) *J. Biol. Chem. 257*, 9849–9854.

Busby, T. F., Atha, D. H., & Ingham, K. C. (1981) *J. Biol. Chem. 256*, 12140–12147.

Castillo, M. J., Nakajima, K., Zimmerman, M., & Powers, J. C. (1979) *Anal. Biochem. 99*, 53–64.

Chesne, S., Villiers, C. L., Arlaud, G. J., LaCroix, M. B., & Colomb, M. G. (1982) *Biochem. J. 201*, 61–70.

Chlebowski, J. F., & Williams, K. (1983) *Biochem. J. 209*, 725–730.

Donaldson, V. H., & Evans, R. R. (1963) *Am. J. Med. 35*, 37–44.

Donovan, J. W. (1969) in *Physical Principals and Techniques of Protein Chemistry. Part A* (Leach, S. J., Ed.) pp

101–170, Academic Press, New York.
Donovan, J. W., & Beardslee, R. A. (1975) *J. Biol. Chem. 250*, 1966–1971.
Franks, F., & Eagland, D. (1975) *CRC Crit. Rev. Biochem. 3*, 165–219.
Freire, E., & Biltonen, R. L. (1978) *Biopolymers 17*, 463–479.
Fuchs, H. E., Shifman, M. A., & Pizzo, S. V. (1982) *Biochim. Biophys. Acta 716*, 151–157.
Gally, J. A., & Edelman, G. M. (1965) *Biochim. Biophys. Acta 94*, 175–182.
Gan, J. C. (1979) *Arch. Biochem. Biophys. 194*, 149–156.
Gonias, S. L., Balber, A. E., Hubbard, W. J., & Pizzo, S. V. (1983) *Biochem. J. 209*, 99–105.
Harpel, P. C., & Cooper, N. R. (1975) *J. Clin. Invest. 55*, 593–604.
Harrison, R. A. (1983) *Biochemistry 22*, 5001–5007.
Haupt, H., Heimberger, N., Kranz, T., & Schwick, H. G. (1970) *Eur. J. Biochem. 17*, 254–261.
Ingham, K. C., Busby, T. F., Atha, D. H., & Forastieri, H. (1983) *J. Liq. Chromatogr. 6*, 229–248.
Kolb, W. P., Kolb, L. M., & Podack, E. R. (1979) *J. Immunol. 122*, 2103–2111.
Laemmli, U. K. (1970) *Nature (London) 227*, 680–685.
Lehrer, S. S. (1971) *Biochemistry 10*, 3254–3263.
Lennick, M., Brew, S. A., & Ingham, K. C. (1983) *Fed. Proc., Fed. Am. Soc. Exp. Biol. 42*, 1951.
McRae, B. J., Lin, T.-Y., & Powers, J. C. (1981) *J. Biol. Chem. 256*, 12362–12366.
Neurath, H. (1984) *Science (Washington, D.C.) 224*, 350–357.
Nilsson, T., & Wiman, B. (1982) *Biochim. Biophys. Acta 705*, 271–276.
Nilsson, T., Sjoholm, I., & Wiman, B. (1983) *Biochem. J. 213*, 617–624.
Odermatt, E., Berger, H., & Sano, Y. (1981) *FEBS Lett. 131*, 283–285.
Ohlsson, K. (1971a) *Scand. J. Clin. Lab. Invest. 28*, 219–223.
Ohlsson, K. (1971b) *Acta Physiol. Scand. 81*, 269–272.
Pace, C. N. (1975) *CRC Crit. Rev. Biochem. 3*, 1–43.
Privalov, P. L. (1979) *Adv. Protein Chem. 33*, 167–241.
Privalov, P. L. (1982) *Adv. Protein Chem. 35*, 1–104.
Privalov, P. L., & Khechinashvili, N. N. (1974) *J. Mol. Biol. 86*, 665–684.
Privalov, P. L., & Medved, L. V. (1982) *J. Mol. Biol. 159*, 665–683.
Shifman, M. A., & Pizzo, S. V. (1982) *J. Biol. Chem. 257*, 3243–3248.
Sim, R. B., Porter, R. R., Reid, K. B. M., & Gigli, I. (1977) *Biochem. J. 163*, 219–227.
Sim, R. B., Reboul, A., Arlaud, G. J., Villiers, C. L., & Colomb, M. G. (1979) *FEBS Lett. 97*, 111–115.
Takahashi, K., & Sturtevant, J. M. (1981) *Biochemistry 20*, 6185–6190.
Tschopp, J., Villiger, W., Fuchs, H., Kilchherr, E., & Engel, J. (1980) *Proc. Natl. Acad. Sci. U.S.A. 77*, 7014–7018.
Villanueva, G. B., & Danishefsky, I. (1979) *Biochemistry 18*, 810–817.
Villanueva, G. B., & Allen, N. (1983) *J. Biol. Chem. 258*, 11010–11013.
Weber, G., & Laurence, D. J. R. (1954) *Biochem. J. 56*, 31.
Weiss, V., & Engel, J. (1983) *Hoppe-Seyler's Z. Physiol. Chem. 364*; 295–301.
Wickerhauser, M. (1980) *J. Meet. 18th Congr. ISH/16th Congr. ISBT Abstr.*, 161.
Wong, R. F., Windwer, S. R., & Feinman, R. D. (1983) *Biochemistry 22*, 3994–3999.
Zahnley, J. C. (1979) *J. Biol. Chem. 254*, 9721–9727.
Zahnley, J. C. (1980) *Biochim. Biophys. Acta 613*, 178–190.
Ziccardi, R. J. (1981) *J. Immunol. 126*, 1769–1773.
Ziccardi, R. J., & Cooper, N. R. (1979) *J. Immunol. 123*, 788–792.